Materials Chemistry and Physics 261 (2021) 124247

Contents lists available at ScienceDirect

Materials Chemistry and Physics

journal homepage: www.elsevier.com/locate/matchemphys

Electrochemical detection of bisphenol a on a MWCNTs/$CuFe_2O_4$ nanocomposite modified glassy carbon electrode

Mehdi Baghayeri [a,*], Amirhassan Amiri [a], Maryam Fayazi [b], Marzieh Nodehi [a], Ali Esmaeelnia [a]

[a] Department of Chemistry, Faculty of Science, Hakim Sabzevari University, PO. Box 397, Sabzevar, Iran
[b] Department of Environment, Institute of Science and High Technology and Environmental Sciences, Graduate University of Advanced Technology, Kerman, Iran

HIGHLIGHTS

- The electrochemical sensor based on MWCNTs/$CuFe_2O_4$ nanocomposite was introduced.
- The oxidation current of bisphenol A on the MWCNTs/$CuFe_2O_4$/GCE sensor increased dramatically.
- The proposed electrochemical sensor showed excellent sensitivity and selectivity.

GRAPHICAL ABSTRACT

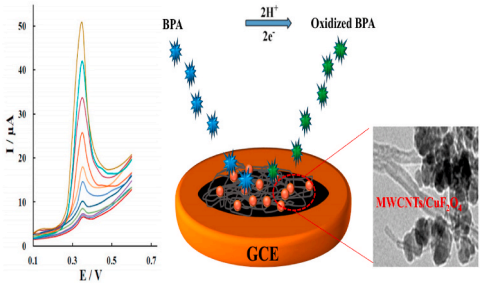

ARTICLE INFO

Keywords:
Bisphenol A
Multi-walled carbon nanotubes
Copper ferrite
Sensor
Nanocomposite

ABSTRACT

In the present study, a novel electrochemical sensor based on glassy carbon electrode (GCE) modified by multi-walled carbon nanotubes/copper ferrite (MWCNTs/$CuFe_2O_4$) nanocomposite was introduced for detection of bisphenol A (BPA). The nanocomposite was prepared by citrate sol-gel method and then characterized using X-ray diffraction (XRD), field emission scanning electron microscopy (FE-SEM), transmission electron microscopy (TEM), and energy-dispersive X-ray (EDX) systems. Electrochemical characterizations of the bare and modified electrodes were explored with cyclic voltammetry (CV) and electrochemical impedance spectroscopy (EIS) methods. Also, the peak current of differential pulse voltammetry (DPV) of BPA was increased linearly with its concentration in the ranges of 0.01–120 μM with a low detection limit of 3.2 nM (S/N = 3). Good selectivity and acceptable reproducibility were also attained on the proposed sensor. Finally, this sensor was successfully employed for the BPA determination in different real samples.

1. Introduction

The normal working hormones and metabolisms indirectly can be affecting by the environment. Different chemical compounds, whether desired or unwanted, are introduced by humans to nature that has a direct impact on the function of hormones. Bisphenol A (BPA, Molecular formula; $C_{15}H_{16}O_2$) is one of the simplest and most important chemical compounds used in making plastic products such as water bottles, food containers, and beverage packages. Widespread use of BPA increases the likelihood of unintended presence in nature. As a dark point, chemical degradation of BPA is very difficult and it has been frequently detected in lots of environmental samples. Finding BPA in natural waters is a

* Corresponding author.
E-mail address: m.baghayeri@hsu.ac.ir (M. Baghayeri).

https://doi.org/10.1016/j.matchemphys.2021.124247
Received 25 October 2020; Received in revised form 4 January 2021; Accepted 4 January 2021
Available online 12 January 2021
0254-0584/

great danger to human health because it is possible to transmit it to various points through water-borne water. Developed countries impose strict rules to prevent the production and sale of BPA containing products. Genital abnormalities in boys [1], decreased sperm count in men [2], earlier sexual maturation in girls [3], and increased breast cancer in women [4] are some of the participation of early BPA exposure in humans. Thus, there is special attention to determine the accurate levels of human and fetal contamination with BPA.

In the last two decades, many studies have been focused on the potential of chromatography methods for the determination of BPA [5,6]. Today, the development of the electrochemical methods has opened a new analytical strategy for the simple and fast detection of BPA [7,8]. Technical advances in the adaptation of the applied electrodes and application of different modifiers often result in analytical improvements for low-cost instruments, accuracy, reliability, and sensitivity in electroanalytical methods [9].

The size and morphology of the modifier and the used fabrication method can be very influential on the electroanalytical response of the designed electrodes. For example, as is common, the effect of increasing surface coverage is considerable when using the nanoparticles (NPs) for modification of electrode surfaces [10]. The use of NPs also improves selectivity, catalytic activity, signal-to-noise ratio, and unique optical properties [11].

Different nanomaterials have been introduced during the development of electrochemical investigations. Transition metal oxides (TMOs) with several oxidation states for oxidation and reduction are successfully utilized as the electrode materials for various electrochemical purposes such as electrochemical energy storage and conversion [12,13], sensing [14,15], and biosensing [16,17] applications. High cost and lack of abundance are two important factors that can restrict the use of different TMOs especially in commercial applications [18]. With low cost, long-term performance, and good stability, and environmentally friendly nature, copper ferrite ($CuFe_2O_4$) can be considered as a promising substitute electrode material for high-performance electrochemical sensing applications [19,20]. However, $CuFe_2O_4$ is well-known as a semiconductor and intrinsically shows low conductivity, which restricts its practical applications in electrochemistry [21]. Some approaches have been suggested to solve these problems. For example, the incorporation of $CuFe_2O_4$ nanostructures into the conducting matrix is a simple and effective way [22]. Carbon nanotubes (CNTs) as the simplest conductive materials can be considered as special candidates for the construction of composites at electro-sensing applications because they have not only high surface area and mechanical stability, but also good electrical conductivity make the excellent conductive nanocomposites [23,24]. Combination of the applicable advantages of $CuFe_2O_4$ nanostructures (biocompatibility and high adsorption ability) [25] beside the exceptional features of multi-walled carbon nanotubes (MWCNTs) (great electrical conductivity and high surface area) [26], the $CuFe_2O_4$/MWCNTs nanocomposite can supply a stable and sensitive platform for electrochemical sensing applications. Up to now, different $CuFe_2O_4$ nanocomposites-based electrodes have been developed for the determination of malathion [27], 3-nitrotyrosine [28], glucose [29] and hydrogen peroxide [30]. However, to the best of our knowledge, $CuFe_2O_4$ nanocomposites have never been applied in BPA detection.

In this paper, MWCNTs/$CuFe_2O_4$ nanocomposite was synthesized by the citrate sol-gel process. By combining the valuable properties of MWCNTs and $CuFe_2O_4$ nanoparticles, a new, simple, and low-cost BPA sensor was proposed. The electroanalytical performance of the modified sensor was studied and presented by various electrochemical methods. The introduced sensor was applied to the analysis of BPA in different real samples with acceptable analytical results.

2. Material and methods

2.1. Apparatus

A Palm Sens Instrumentation (Palm Instrument BV, the Netherlands) was used in all electrochemical measurements. The electrochemical cell consisted of a glassy carbon electrode (GCE), uses as the working electrode (3 mm diameter, Azar electrode, Iran), a platinum wire, as the counter electrode, and a Ag|AgCl|KCl (3 M) as the reference electrode. Electrochemical impedance spectroscopy (EIS) data was obtained in 5.0 mM $K_3Fe(CN)_6/K_4Fe(CN)_6$ (1/1) mixture with 0.1 M KCl as supporting electrolyte, using an alternating current voltage of 5 mV, within the frequency range of 0.1–10^5 Hz.

2.2. Reagents

Sodium hydroxide (NaOH), potassium chloride (KCl), potassium dihydrogen phosphate (KH_2PO_4), dipotassium hydrogen phosphate (K_2HPO_4), hydrochloric acid (HCl), copper (II) nitrate trihydrate ($Cu(NO_3)_2.3H_2O$), iron (III) nitrate nonahydrate ($Fe(NO_3)_3.9H_2O$) and citric acid used in this work was obtained from Merck. BPA was purchased from Merck chemical company and solutions were freshly prepared before electrochemical tests. Pristine MWCNTs (>95%, O.D.: 10–15 nm, I.D.: 2–6 nm, length: 0.1–10 μm) were obtained from Sigma-Aldrich company. All other chemicals were of analytical grade and were used as received without any purification and solutions were prepared with deionized water. 0.1 M phosphate buffer solutions (PBS) were prepared using KH_2PO_4 and K_2HPO_4 salts and adjusting the pH was performed with HCl and NaOH solutions.

2.3. Synthesis process

Before synthesize of MWCNTs/$CuFe_2O_4$ nanocomposite, raw MWCNTs were treated with concentrated HNO_3 to cause segmentation and carboxylation. In addition, the oxidation of MWCNTs can significantly promote the interaction between MWCNTs and iron and copper ions. The details of the modification procedure are described in Ref. [31]. MWCNTs/$CuFe_2O_4$ nanocomposite was successfully fabricated through the citrate sol-gel method. In a typical experiment, 5.0 mmol $Cu(NO_3)_2.3H_2O$ and 10.0 mmol $Fe(NO_3)_3.9H_2O$ were dissolved in 60.0 mL deionized water. 18.0 mmol of citric acid was added to the mixture and then magnetically stirred at 80 °C for 3 h. In the next step, 1.0 g of MWCNTs added to the above mixture, and the mixture was sonicated in an ultrasonic bath at 80 °C for 1 h. After evaporation of the excess water at 80 °C, the prepared gel was dried overnight in an oven at 120 °C and then calcined at 400 °C for 4 h under air condition. The product was grinded and washed several times in excess water and dried at 80 °C for 24 h before electrochemical tests. In addition, the $CuFe_2O_4$ particles were prepared by the similar procedure without the MWCNTs.

2.4. Preparation of sensor

Following conventional pretreatment protocol [32], the bare GCE was firstly cleaned for utilization in the next modification step. Then, 1.0 mg of MWCNTs/$CuFe_2O_4$ was well dispersed in 1.0 mL of ethanol by the ultrasonic bath at room temperature for 10 min until a homogenous black dispersion was obtained. The MWCNTs/$CuFe_2O_4$ suspension (5 μL) was dropped on the clean GCE surface and allowed to dry for 20 min at room temperature.

3. Results and discussion

3.1. Characterization of $CuFe_2O_4$ nanoparticles and MWCNTs/$CuFe_2O_4$ nanocomposite

The crystal structure of $CuFe_2O_4$ nanoparticles and MWCNTs/

$CuFe_2O_4$ nanocomposite were investigated using the X-ray diffraction pattern. As can be seen from Fig. 1, the diffraction peak at $2\theta = 26.3^\circ$ is ascribed to (002) reflections of MWCNTs [33]. Also, diffraction peaks at 2θ values of 30.4°, 35.8°, 43.6°, 57.3°, and 62.9° can be indexed respectively to the (220), (311), (400), (511) and (440) planes of the cubic phase of $CuFe_2O_4$ particles (JCPDS Card No. 25–0283) [34]. The morphology and the size of the prepared materials were characterized by FE-SEM and TEM. According to Fig. S1, $CuFe_2O_4$ nanoparticles presents a spherical morphology with an average diameter of 47 nm (n = 40). In MWCNTs/$CuFe_2O_4$ sample (Fig. 2), the MWCNTs have a tubular structure and the spherical $CuFe_2O_4$ nanoparticles are well placed on the surface of the MWCNTs with an average diameter of 32 nm (n = 40). As a result, the loading of $CuFe_2O_4$ on MWCNTs reduces the size of particles to expose more active sites in the nanocomposite. The surface composition of the product was investigated with an energy-dispersive X-ray (EDX) system. The EDX spectra of both $CuFe_2O_4$ and MWCNTs/$CuFe_2O_4$ materials depicted in Fig. S2. As seen, the spectrum of the prepared nanocomposite demonstrates the presence of Cu, C, Fe, and O elements. All above results demonstrate that the MWCNTs/$CuFe_2O_4$ modifier has been successfully prepared via the citrate sol-gel process.

3.2. Electrochemical properties of the sensor

Cyclic voltammetry (CV) and EIS were used to characterize the electrochemical performance of the modified electrode in a redox probe solution containing 5 mM $Fe(CN)_6^{3-/4-}$ + 0.1 M KCl. According to CV studies in Fig. 3A, the bare GCE and modified electrodes exhibit well-defined anodic and cathodic peaks corresponding to the expected electrochemical behavior of redox couples. Correspond to expectations; the catalytic capacity of $CuFe_2O_4$ nanoparticles accelerates the electrochemical reaction process of the probe at the surface of $CuFe_2O_4$/GCE. For MWCNTs/$CuFe_2O_4$/GCE, the peak current increased compared with the other two studied electrodes due to the synergistic effect of the $CuFe_2O_4$ and MWCNTs in the prepared nanocomposite.

The electrochemical performance of the modified electrodes was also investigated using EIS studies (Fig. 3B). For the bare GCE, the value of electron transfer resistance (R_{et}) is 1878.3 Ω, revealing a large semicircle arc. After immobilization of $CuFe_2O_4$ nanoparticles, the value of R_{et} decrease from 1878.3 Ω to 1030.0 Ω. The results showed that the presence of $CuFe_2O_4$ nanoparticles could facilitate the electron transfer between the probe and $CuFe_2O_4$/GCE. For MWCNTs/$CuFe_2O_4$/GCE, the semicircle diameter decreased to 549.5 Ω, suggesting that the synergistic effects of MWCNTs and $CuFe_2O_4$ nanoparticles in the composite film resulted in the good electron transfer rate with the decrease of the

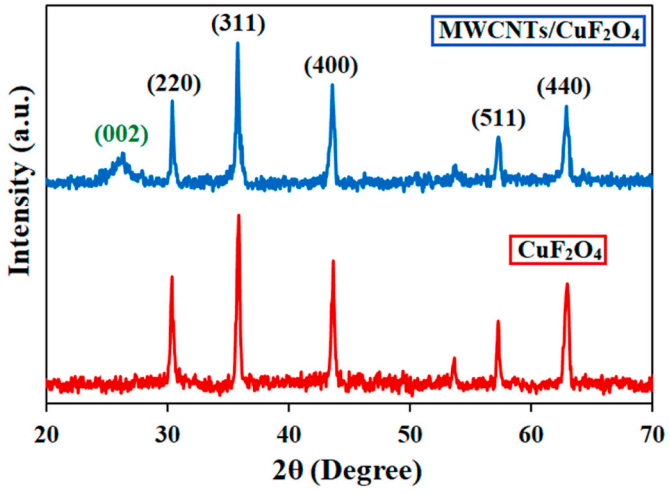

Fig. 1. XRD patterns of $CuFe_2O_4$ nanoparticles and MWCNTs/$CuFe_2O_4$ nanocomposite.

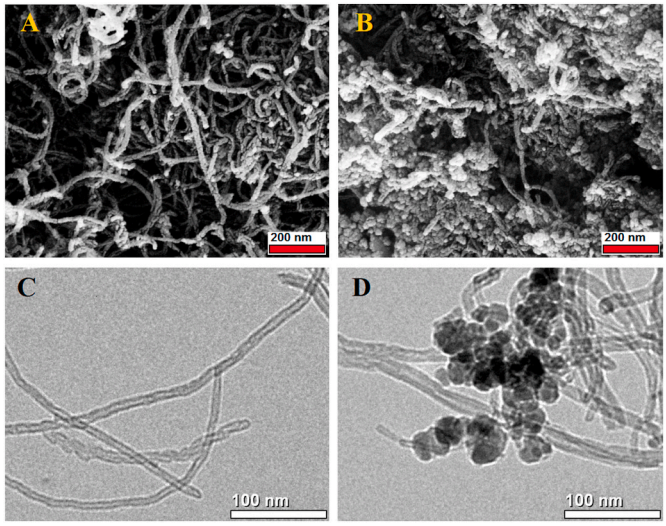

Fig. 2. (A and B) FE-SEM and (C and D) TEM images of MWCNTs and MWCNTs/$CuFe_2O_4$ nanocomposite.

R_{et} value. The results of EIS are in good agreement with the above CV experiments.

3.3. Initial investigations on BPA detection

To comprehend the electrochemical performance of BPA at bare and various modified GCE, its individual cyclic voltammograms were studied first in 0.1 M PBS (pH 7.0) at a scan rate of 100 mVs^{-1}. As shown in Fig. 4A, BPA signal is recognizable as an irreversible small oxidation peak at 0.45 V on the bare GCE, which proves the slow electron transfer kinetics of BPA oxidation process [35]. It could also be seen from Figure that BPA oxidation on $CuFe_2O_4$/GCE exhibited 5.6-fold larger peak current than bare GCE at the almost same potential. However, the electro-oxidation of BPA on the MWCNTs/$CuFe_2O_4$/GCE revealed a sharp anodic peak at 0.39 V and the anodic peak current was enhanced by about 13.2 folds in comparison with the anodic peak current on the bare GCE. As compared to the unmodified GCE, the detected 60 mV negative shift and improved anodic current for the oxidation of BPA at the MWCNTs/$CuFe_2O_4$/GCE showed that the MWCNTs/$CuFe_2O_4$ modifier has excellent electrocatalytic activity toward the oxidation of BPA.

3.4. Effect of pH on the electrochemical behavior of BPA

Because of the presence of two phenol functional groups at the structure of BPA, the redox reaction of BPA largely depends on the changes in the pH of the solution. Fig. 4B investigates the effect of solution pH on the anodic peak current and potential of 100 μM BPA in 0.1 M PBS by CV. As can be seen, the oxidation current increased with an increasing pH value from 5.0 to 9.0, and the maximum value of anodic current appeared at pH 7.0. Furthermore, anodic peak potential changes negatively, from pH 5.0 to 9.0, with resulted equation $E = 0.872–0.0586$ pH, which is linear and presents a slope close to the Nernstian value −0.0586 V/pH, suggesting that an equal number of protons and electrons participate at electrochemical reaction [36], and the possible oxidation process was presented in Scheme 1.

3.5. Effect of scan rate

The influence of scan rate (υ) on the electroanalytical response of 100 μM BPA in 0.1 M PBS (pH 7.0) at the modified electrode was examined by CV, and the voltammograms are presented in Fig. 5. As shown in the inset of Fig. 3, the oxidation peak current of BPA linearly increased with the scan rate in the range from 10 to 250 mVs^{-1},

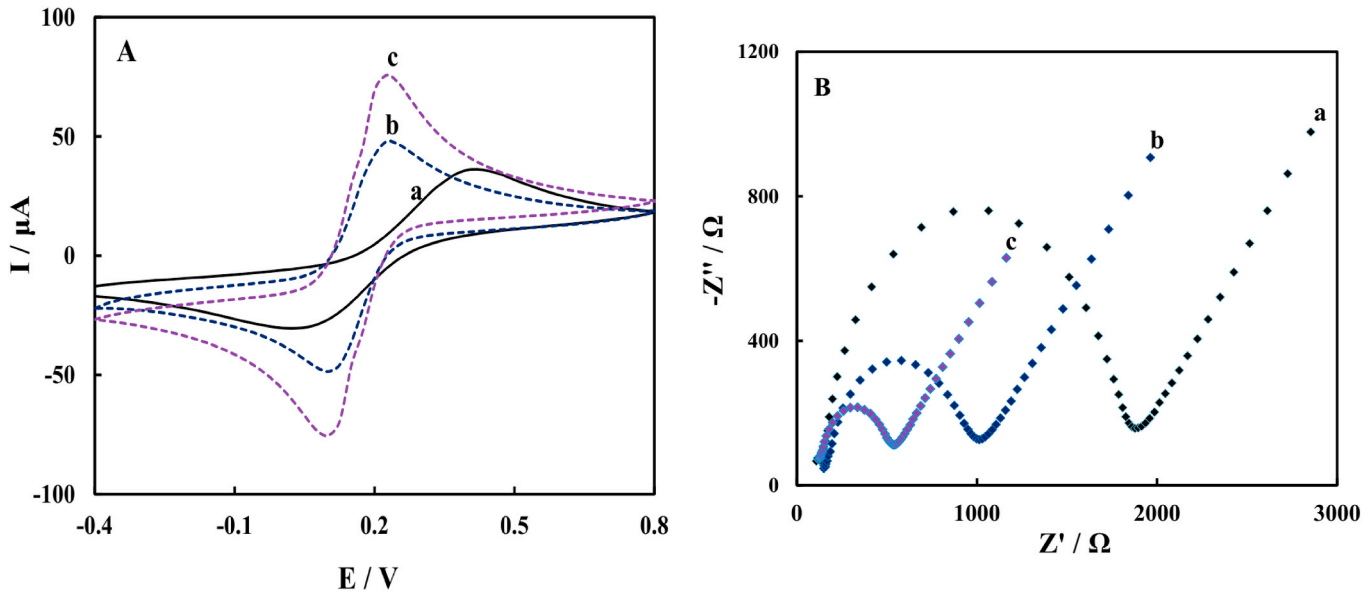

Fig. 3. (A) Cyclic voltammograms of (a) bare GCE, (b) $CuFe_2O_4$/GCE and (c) MWCNTs/$CuFe_2O_4$/GCE in 5 mM $Fe(CN)_6^{3-/4-}$ (1:1) solution containing 0.1 M KCl at a scan rate of 100 mVs^{-1}. (B) Nyquist plot of EIS for (a) bare GCE, (b) $CuFe_2O_4$/GCE and (c) MWCNTs/$CuFe_2O_4$/GCE.

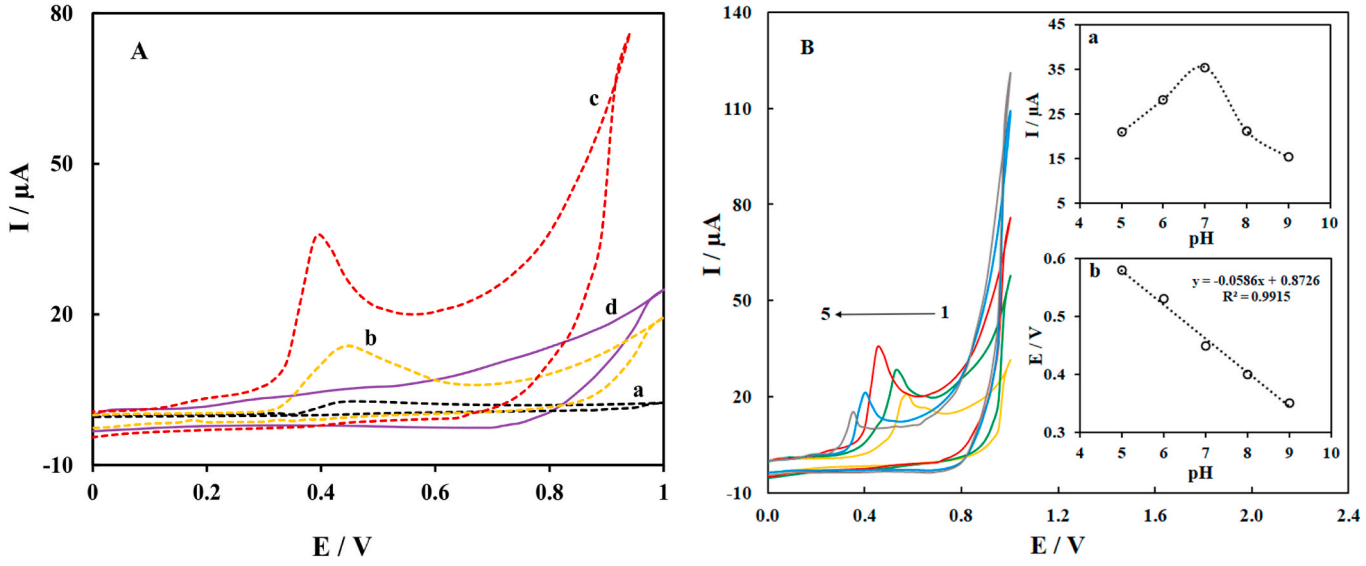

Fig. 4. (A) CVs of different electrodes in 0.1 M PBS (pH 7.0) containing 100 μM BPA (a) GCE, (b) $CuFe_2O_4$/GCE, (c) MWCNTs/$CuFe_2O_4$/GCE at a scan rate 100 mVs^{-1}. Curve d: the CV of MWCNTs/$CuFe_2O_4$/GCE in 0.1 M PBS (pH 7.0) without BPA. (B) Cyclic voltammograms of MWCNTs/$CuFe_2O_4$/GCE in 100.0 μM BPA solution at different pH values (curve 1–5, 5.0 (yellow curve), 6.0 (green curve), 7.0 (red curve), 8.0 (blue curve) and 9.0 (gray curve)); scan rate 100 mVs^{-1}. Inset a: Dependence of the peak current on the pH. Inset b: Influence of the solution pH on the peak potential. (For interpretation of the references to colour in this figure legend, the reader is referred to the Web version of this article.)

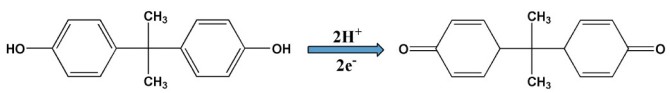

Scheme 1. The possible electrooxidation of BPA at MWCNTs/$CuFe_2O_4$/GCE.

suggesting that the electrooxidation of BPA at MWCNTs/$CuFe_2O_4$/GCE controls by adsorption process [37]. A straight line with a slope of 0.9964 (Fig. S3) is obtained after the plotting of the logarithm of oxidation peak current versus the logarithm of the scan rate, which is close to the theoretical value of 1.0 and expresses an ideal reaction for the adsorption-controlled electrode process [38].

3.6. Performance of MWCNTs/$CuFe_2O_4$/GCE for BPA determination

The quantitative performance of the modified electrode for analysis of BPA was studied by DPV at the obtained optimum condition. As shown in Fig. 6A, the anodic current of BPA increases linearly with increasing concentration in the range of 0.01–120 μM while the linear equation is calculated to be $I_P = 0.3563C + 7.6438$ ($R^2 = 0.9967$). The detection limit was 3.2 nM based on three times the background noise. The MWCNTs/$CuFe_2O_4$/GCE showed good reproducibility and the relative standard deviation (R.S.D.) was 4.1%, which was evaluated by ten repetitive measurements of 50 μM BPA. The stability of the proposed sensor is also studied. The modified electrode lost only 5.2% of the initial anodic response for 50 μM BPA after storage for 3 weeks, which

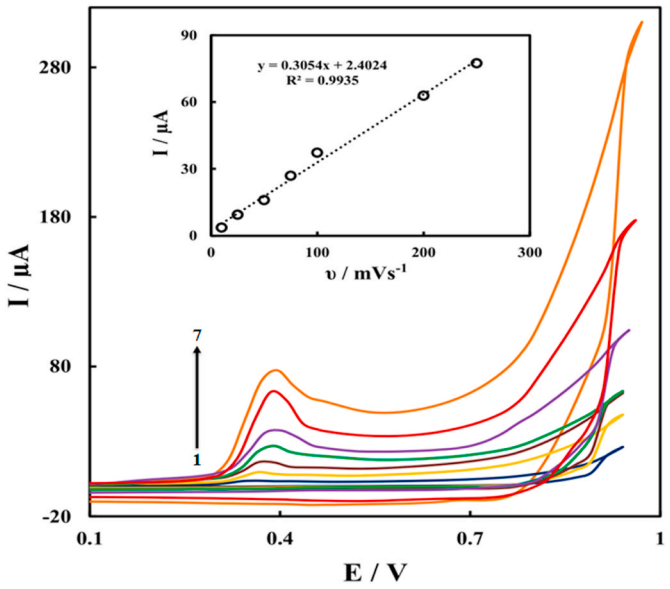

Fig. 5. CVs of 100 µM BPA at various scan rates: (1) 10, (2) 25, (3) 50, (4) 75, (5) 100, (6) 200, and (7) 250 mV s^{-1} in 0.1 M PBS (pH 7.0) at MWCNTs/$CuFe_2O_4$/GCE. Inset: plot of anodic peak current versus scan rate.

can be a reason for the excellent stability of the nanocomposite. Some characteristic parameters such as the detection method, pH of detection, linear range, sensitivity, and the limit of detection of other reported sensors [39–52] are summarized in Table 1. These results indicated that the suggested MWCNTs/$CuFe_2O_4$ nanocomposite is an excellent platform for the detection of BPA.

3.7. Interference study and analytical application

In human epidemiological studies, BPA exposure predominantly is measurable via urinary concentrations. Also, in the studies for environmentally relevant exposure, some biological effects are measurable via the determination of BPA dosage in water samples. Therefore, investigation of the anti-interference ability of the MWCNTs/$CuFe_2O_4$/GCE is very important. The potential interference for the detection of BPA on the proposed sensor was examined by the addition of various inorganic ions, such as 100-fold concentration K^+, Na^+, Mg^{2+}, Zn^{2+}, NH_4^+, F^-, Cl^-, NO_3^-, SO_4^{2-}, CO_3^{2-} into the experimental solution containing 50 µM BPA. All the above inorganic ions caused no interference to the detection of BPA with the peak current changes less than ±5%. Also, the oxidation potential of many phenolic compounds such as *p*-nitrophenol, *o*-nitrophenol, and catechol is not located in the studied potential range and does not restrict the detection of BPA. Furthermore, for the 100-fold concentration of glucose, fructose, lactose, urea, and sucrose changes of anodic currents are less than 5%, revealing no influence on BPA determination (Fig. 6B). These results revealed that the prepared electrode has an excellent ability to detect BPA at various real samples.

3.8. Evaluation performance

Practical applications of the proposed sensor were evaluated in the real samples (water and baby bottles) by using DPV method. The baby bottle samples were prepared for the experiment as follows: the baby bottle was cleaned with acetone and rinsed several times with doubly distilled water. The dried baby bottle cut into small pieces and 1.0 g of it poured into a 500 mL beaker containing chloroform (100 mL). The small pieces were dissolved in chloroform using an ultrasonic bath. Then, 200 mL of 0.5 M sodium hydroxide as an extraction solvent was added to the beaker. After three times of extraction, the extract solution was collected, diluted with double distilled water, and used for detection of BPA content. The analytical performance of the sensor was evaluated by the standard addition method. The results are collected in Table 2.

4. Conclusion

A simple and perfect electrochemical sensor for the detection of BPA was constructed based on the citrate sol-gel prepared MWCNTs/$CuFe_2O_4$ nanocomposite. It is demonstrated that the synthesized nanocomposite has a positive influence on the electroanalytical signal of the BPA. The proposed sensor has good sensitivity and selectivity. The MWCNTs/$CuFe_2O_4$/GCE was successfully applied in determining BPA in

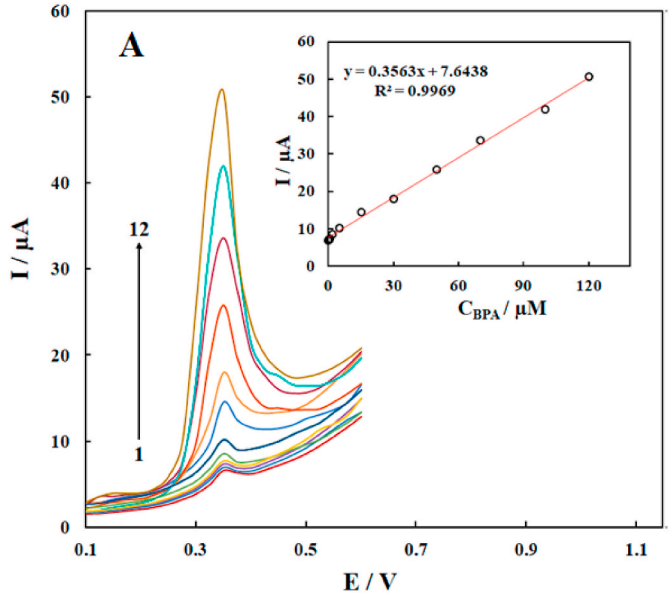

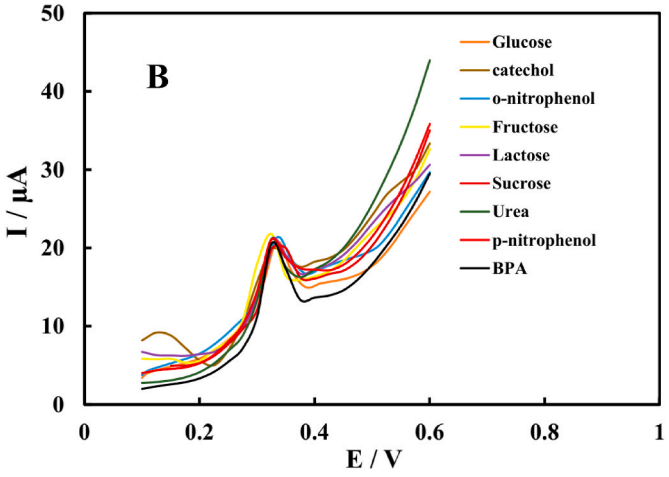

Fig. 6. (A) Differential pulse voltammograms of MWCNTs/$CuFe_2O_4$/GCE in 0.1 M PBS (pH 7.0) containing different concentrations of BPA: (1) 0.01, (2) 0.08, (3) 0.2, (4) 0.7, (5) 2.0, (6) 5.0, (7) 15.0, (8) 30.0, (9) 50.0, (10) 70.0, (11) 100.0 and (12) 120.0 µM. Inset: plot of the peak current as a function of BPA concentrations. (B) Differential pulse voltammograms of MWCNTs/$CuFe_2O_4$/GCE in 0.1 M PBS (pH 7.0) containing 50 µM BPA in the presence of same concentration of *p*-notrophenol, *o*-nitrophenol and catchol, and 100-fold of glucose, fructose, lactose, urea, and sucrose compounds.

Table 1
Comparison of some BPA electrochemical sensors.

Modified electrode	Detection method	pH	Liner range (μM)	LOD (nM)	Sensitivity (μA/μM)	Real sample	References
SH-β-CD/NPGL/GE[a]	SWV	7.0	0.3–100	60.0	4.8	Water, milk	[39]
AuNPs-GO-CTS-ECH/GCE[b]	SWV	7.0	0.95–140	280.0	4.8×10^4	Water	[40]
NiO/MWCNT/GCE[c]	DPV	6.0	2.4–46	59.0	5.3	Water	[41]
ZnTsPc/f-GN/GCE[d]	DPV	7.0	0.05–4	20.0	0.755	Drinking bottles	[42]
TYR–TiO_2–MWCNTs–PDDA–Nafion/GE[e]	Amperometry	6.0	0.28–45.05	66.0	9.137	Plastic bag for rice	[43]
RGO-Ag/PLL/GCE[f]	DPV	8.0	1–80	540.0	0.733,0.157	Water	[44]
CNT/GCE[g]	Amperometry	7.0	0.3–100	98.0	–	Water	[45]
CMK-3/nano-CILPE[h]	LSV	7.0	0.2–150	50	0.774	Polycarbonate drinking bottle	[46]
Na-doped WO_3/CPE[i]	DPV	7.0	0.0810–22.5	28.0	0.3105	Water, milk	[47]
Cu_2O-rGO/GCE[j]	Amperometry	6.5	0.1–80.0	53.0	0.0035	Water	[48]
PEI-PC/DPNs/AuNPs/SPCE[k]	Amperometry	7.4	0.01-1,1-300	6.6	0.0298	Water	[49]
AuPdNPs/GNs/GCE[l]	DPV	7.5	0.05–10	8.0	3.97	Food package	[50]
MCM-41/CPE[m]	DPV	8.0	0.22–8.8	38.0	2.833	Water	[51]
ILs-LDH/GCE[n]	DPV	8.0	0.01–3.0	4.6	2.17	Water	[52]
MWCNTs/$CuFe_2O_4$/GCE	DPV	7.0	0.01–120	3.2	0.355	Water and baby bottles	This work

[a] Thiolated beta-cyclodextrin/Nano porous gold leaf/gold electrode.
[b] Gold Nano particles-graphene oxide-crosslinked chitosan-epichlorohydrin/glassy carbon electrode.
[c] Nickel oxide nanoparticles/multi-walled carbon nanotubes/glassy carbon electrode.
[d] zinc phthalocyanine tetrasulfonic acid/functionalized graphene nanocomposites/glassy carbon electrode.
[e] Tyrosinase- TiO2- multi-walled carbon nanotubes-polycationic polymer poly (diallyldimethylammonium chloride)- Nafion/graphite electrode.
[f] Reduced graphene oxide-silver/poly-L-lysine nanocomposites/glassy carbon electrode.
[g] carbon nanotube/glassy carbon electrode.
[h] Mesoporous carbon CMK-3 modified Nano-carbon ionic liquid paste electrode (CMK-3/Nano-CILPE).
[i] Na-doped WO_3 nanorods/carbon paste electrode/Au nanoparticles.
[j] cuprous oxide-reduction of graphene oxide/glassy carbon electrode.
[k] polyethyleneimine-phosphatidylcholine/dendritic platinum nanoparticles/Au nanoparticles/screen-printed carbon electrode.
[l] AuPd nanoparticles/graphene nanosheets/glassy carbon electrode.
[m] MCM-41, (a kind of mesoporous silica)/carbon paste electrode.
[n] 1-aminopropyl-3-methylimidzaolium tetrafluoroborate/glassy carbon electrode.

Table 2
Determination of BPA in various real samples (n = 5).

Sample	Added (μM)	Found (μM)	RSD (%)	Recovery (%)
1	0	3.32 (±0.08)	2.4	–
	0.5	3.81 (±0.14)	3.8	99.7
	1	4.31 (±0.19)	4.4	99.7
2	0	5.32 (±0.27)	5.1	–
	5	10.41 (±0.27)	2.6	100.8
	10	14.98 (±0.66)	4.4	97.7
3	0	3.63 (±0.12)	3.4	–
	15	18.68 (±0.34)	1.8	100.2
	30	33.39 (±0.70)	2.1	99.2
4	0	–	–	–
	5	4.79 (±0.14)	2.9	95.8
	10	10.31 (±0.39)	3.8	103.1
5	0	–	–	–
	30	29.49 (±1.36)	4.6	98.3
	50	48.70 (±1.22)	2.5	97.4

1,2 and 3: Baby bottles samples, 4: Tap water, Sabzevar, Iran, 5: Mineral water (Damavand Co., Iran).

real plastic and water samples with recovery ranging from 95.8% to 103.1%. The fabricated sensor showed remarkable selectivity, stability, and reproducibility.

CRediT authorship contribution statement

Mehdi Baghayeri: Project administration, Supervision, Conceptualization. **Amirhassan Amiri:** Methodology, Validation. **Maryam Fayazi:** Resources, Investigation. **Marzieh Nodehi:** Writing - original draft, Writing - review & editing, Data curation. **Ali Esmaeelnia:** Investigation, Formal analysis.

Declaration of competing interest

The authors declare that they have no known competing financial interests or personal relationships that could have appeared to influence the work reported in this paper.

Acknowledgment

We would like to thank the post-graduate office of Hakim Sabzevari University for the support of this work.

Appendix A. Supplementary data

Supplementary data to this article can be found online at https://doi.org/10.1016/j.matchemphys.2021.124247.

References

[1] L.J. Paulozzi, J.D. Erickson, R.J. Jackson, Hypospadias trends in two US surveillance systems, Pediatrics 100 (1997) 831–834.
[2] E. Carlsen, A. Giwercman, N. Keiding, N.E. Skakkebæk, Evidence for decreasing quality of semen during past 50 years, Br. Med. J. 305 (1992) 609–613.
[3] M.E. Herman-Giddens, E.J. Slora, R.C. Wasserman, C.J. Bourdony, M.V. Bhapkar, G.G. Koch, C.M. Hasemeier, Secondary sexual characteristics and menses in young girls seen in office practice: a study from the Pediatric Research in Office Settings network, Pediatrics 99 (1997) 505–512.
[4] A. Brewster, K. Helzlsouer, Breast cancer epidemiology, prevention, and early detection, Curr. Opin. Oncol. 13 (2001) 420–425.
[5] N.Y. Polovkov, J. Starkova, R. Borisov, A simple, inexpensive, non-enzymatic microwave-assisted method for determining bisphenol-A in urine in the form of trimethylsilyl derivative by GC/MS with single quadrupole, J. Pharm. Biomed. (2020) 113417.
[6] M. Háková, L.C. Havlíková, J. Chvojka, P. Solich, D. Šatínský, An on-line coupling of nanofibrous extraction with column-switching high performance liquid chromatography–A case study on the determination of bisphenol A in environmental water samples, Talanta 178 (2018) 141–146.
[7] S. Zhang, Y. Shi, J. Wang, L. Xiao, X. Yang, R. Cui, Z. Han, Nanocomposites consisting of nanoporous platinum-silicon and graphene for electrochemical determination of bisphenol A, Microchim. Acta 187 (2020) 1–8.

[8] D. Jemmeli, E. Marcoccio, D. Moscone, C. Dridi, F. Arduini, Highly Sensitive Paper-Based Electrochemical Sensor for a Reagent Free Detection of Bisphenol A, 2020, p. 120924. Talanta.

[9] G.F. Pereira, L.S. Andrade, R.C. Rocha-Filho, N. Bocchi, S.R. Biaggio, Electrochemical determination of bisphenol A using a boron-doped diamond electrode, Electrochim. Acta 82 (2012) 3–8.

[10] F.W. Campbell, R.G. Compton, The use of nanoparticles in electroanalysis: an updated review, Anal. Bioanal. Chem. 396 (2010) 241–259.

[11] M. Baghayeri, R. Ansari, M. Nodehi, I. Razavipanah, H. Veisi, Voltammetric aptasensor for bisphenol A based on the use of a MWCNT/Fe_3O_4@ gold nanocomposite, Microchim. Acta 185 (2018) 320.

[12] G. Patrinoiu, V. Etacheri, S. Somacescu, V.S. Teodorescu, R. Birjega, D.C. Culita, C. N. Hong, J.M. Calderon-Moreno, V.G. Pol, O. Carp, Spherical cobalt/cobalt oxide-Carbon composite anodes for enhanced lithium-ion storage, Electrochim. Acta 264 (2018) 191–202.

[13] L. Thirugunanam, S. Kaveri, V. Etacheri, S. Ramaprabhu, M. Dutta, V.G. Pol, Electrospun nanoporous TiO2 nanofibers wrapped with reduced graphene oxide for enhanced and rapid lithium-ion storage, Mater. Char. 131 (2017) 64–71.

[14] M. Ghanei-Motlagh, M.A. Taher, M. Fayazi, M. Baghayeri, A. Hosseinifar, Non-enzymatic amperometric sensing of hydrogen peroxide based on vanadium pentoxide nanostructures, J. Electrochem. Soc. 166 (2019) B367.

[15] M. Baghayeri, A. Amiri, Z. Alizadeh, H. Veisi, E. Hasheminejad, Non-enzymatic voltammetric glucose sensor made of ternary NiO/Fe_3O_4-SH/para-amino hippuric acid nanocomposite, J. Electroanal. Chem. 810 (2018) 69–77.

[16] M. Baghayeri, H. Veisi, M. Ghanei-Motlagh, Amperometric glucose biosensor based on immobilization of glucose oxidase on a magnetic glassy carbon electrode modified with a novel magnetic nanocomposite, Sensor. Actuator. B Chem. 249 (2017) 321–330.

[17] Z. Zhang, S. Zhang, L. He, D. Peng, F. Yan, M. Wang, J. Zhao, H. Zhang, S. Fang, Feasible electrochemical biosensor based on plasma polymerization-assisted composite of polyacrylic acid and hollow TiO2 spheres for sensitively detecting lysozyme, Biosens. Bioelectron. 74 (2015) 384–390.

[18] C. Yuan, H.B. Wu, Y. Xie, X.W. Lou, Mixed transition-metal oxides: design, synthesis, and energy-related applications, Angew. Chem. Int. Ed. 53 (2014) 1488–1504.

[19] R. Bavandpour, H. Karimi-Maleh, M. Asif, V.K. Gupta, N. Atar, M. Abbasghorbani, Liquid phase determination of adrenaline uses a voltammetric sensor employing CuFe2O4 nanoparticles and room temperature ionic liquids, J. Mol. Liq. 213 (2016) 369–373.

[20] H. Xia, J. Li, L. Ma, Q. Liu, J. Wang, Electrospun porous $CuFe_2O_4$ nanotubes on nickel foam for nonenzymatic voltammetric determination of glucose and hydrogen peroxide, J. Alloys Compd. 739 (2018) 764–770.

[21] M. Baghayeri, R. Ansari, M. Nodehi, I. Razavipanah, H. Veisi, Label-free electrochemical bisphenol A aptasensor based on designing and fabrication of a magnetic gold nanocomposite, Electroanalysis 30 (2018) 2160–2166.

[22] K. Atacan, $CuFe_2O_4$/reduced graphene oxide nanocomposite decorated with gold nanoparticles as a new electrochemical sensor material for L-cysteine detection, J. Alloys Compd. 791 (2019) 391–401.

[23] Y. Zhang, E. Zhou, Y. Li, X. He, A novel nonenzymatic glucose sensor based on magnetic copper ferrite immobilized on multiwalled carbon nanotubes, Anal. Methods 7 (2015) 2360–2366.

[24] H. Karimi-Maleh, M. Alizadeh, Y. Orooji, F. Karimi, M. Baghayeri, J. Rouhi, S. Tajik, H. Beitollahi, S. Agarwal, V.K. Gupta, S. Rajendran, S. Rostamnia, L. Fu, F. Saberi-Movahed, S. Malekmohammadi, Guanine-Based DNA Biosensor Amplified with Pt/SWCNTs Nanocomposite as Analytical Tool for Nanomolar Determination of Daunorubicin as an Anticancer Drug: A Docking/Experimental Investigation, Ind. Eng. Chem. Res. (2021). In press, https://dx.doi.org/10.1021/acs.iecr.0c04698.

[25] Z. Xu, X. Lyu, B. Yang, W. Cao, R. Li, X. Zhang, X. Zhang, G. Fan, X. Kong, Q. Liu, Meso-tetrakis (4-chlorophenyl) porphyrin functionalized $CuFe_2O_4$/SiO_2 nanocomposites with enhanced peroxidase-like activity conveniently using for visual biosensing at room temperature, Colloids Surf. A Physicochem. Eng. Asp. 569 (2019) 28–34.

[26] A. Wong, M. Scontri, E.M. Materon, M.R. Lanza, M.D. Sotomayor, Development and application of an electrochemical sensor modified with multi-walled carbon nanotubes and graphene oxide for the sensitive and selective detection of tetracycline, J. Electroanal. Chem. 757 (2015) 250–257.

[27] G.A.T. Battad, J.G. Estacio, J.L.C. Indiongco, M. Mopon Jr., Development of a $CuFe_2O_4$-Reduced graphene oxide-based electrochemical sensor for malathion, key engineering materials, Trans Tech. Publ. (2020) 41–47.

[28] S.-M. Chen, R. Umamaheswari, G. Mani, T.-W. Chen, M.A. Ali, A.-H. Fahad, M. Elshikh, M.A. Farah, Hierarchically structured $CuFe_2O_4$ ND@RGO composite for the detection of oxidative stress biomarker in biological fluids, Inorg. Chem. Front. 5 (2018) 944–950.

[29] Z. Shahnavaz, F. Lorestani, W.P. Meng, Y. Alias, Core-shell–$CuFe_2O_4$/PPy nanocomposite enzyme-free sensor for detection of glucose, J. Solid State Electrochem. 19 (2015) 1223–1233.

[30] C. Karthikeyan, K. Ramachandran, S. Sheet, D.J. Yoo, Y.S. Lee, Y. Satish Kumar, A. R. Kim, G. Gnana Kumar, Pigeon-excreta-mediated synthesis of reduced graphene oxide (rGO)/$CuFe_2O_4$ nanocomposite and its catalytic activity toward sensitive and selective hydrogen peroxide detection, ACS Sustain. Chem. Eng. 5 (2017) 4897–4905.

[31] M. Fayazi, Removal of mercury (II) from wastewater using a new and effective composite: sulfur-coated magnetic carbon nanotubes, Environ. Sci. Pollut. Res. (2020) 1–10.

[32] M. Ghanei-Motlagh, M.A. Taher, A. Heydari, R. Ghanei-Motlagh, V.K. Gupta, A novel voltammetric sensor for sensitive detection of mercury (II) ions using glassy carbon electrode modified with graphene-based ion imprinted polymer, Mater. Sci. Eng. C 63 (2016) 367–375.

[33] M. Fayazi, M.A. Taher, D. Afzali, A. Mostafavi, M. Ghanei-Motlagh, Synthesis and application of novel ion-imprinted polymer coated magnetic multi-walled carbon nanotubes for selective solid phase extraction of lead (II) ions, Mater. Sci. Eng. C 60 (2016) 365–373.

[34] T.-W. Chen, S. Chinnapaiyan, S.-M. Chen, M. Ajmal Ali, M.S. Elshikh, A. Hossam Mahmoud, Facile synthesis of copper ferrite nanoparticles with chitosan composite for high-performance electrochemical sensor, Ultrason. Sonochem. 63 (2020) 104902.

[35] H. Li, W. Wang, Q. Lv, G. Xi, H. Bai, Q. Zhang, Disposable paper-based electrochemical sensor based on stacked gold nanoparticles supported carbon nanotubes for the determination of bisphenol A, Electrochem. Commun. 68 (2016) 104–107.

[36] Q. Liu, X. Kang, L. Xing, Z. Ye, Y. Yang, A facile synthesis of nanostructured $CoFe_2O_4$ for the electrochemical sensing of bisphenol A, RSC Adv. 10 (2020) 6156–6162.

[37] H. Yin, Y. Zhou, J. Xu, S. Ai, L. Cui, L. Zhu, Amperometric biosensor based on tyrosinase immobilized onto multiwalled carbon nanotubes-cobalt phthalocyanine-silk fibroin film and its application to determine bisphenol A, Anal. Chim. Acta 659 (2010) 144–150.

[38] J.N. Soderberg, A.C. Co, A.H.C. Sirk, V.I. Birss, Impact of porous electrode properties on the electrochemical transfer coefficient, J. Phys. Chem. B 110 (2006) 10401–10410.

[39] R. Zhang, Y. Zhang, X. Deng, S. Sun, Y. Li, A novel dual-signal electrochemical sensor for bisphenol A determination by coupling nanoporous gold leaf and self-assembled cyclodextrin, Electrochim. Acta 271 (2018) 417–424.

[40] A. Wong, C.A. Razzino, T.A. Silva, O. Fatibello-Filho, Square-wave voltammetric determination of clindamycin using a glassy carbon electrode modified with graphene oxide and gold nanoparticles within a crosslinked chitosan film, Sensor. Actuator. B Chem. 231 (2016) 183–193.

[41] L.A. Goulart, L.H. Mascaro, GC electrode modified with carbon nanotubes and NiO for the simultaneous determination of bisphenol A, hydroquinone and catechol, Electrochim. Acta 196 (2016) 48–55.

[42] K. Hou, L. Huang, Y. Qi, C. Huang, H. Pan, M. Du, A bisphenol A sensor based on novel self-assembly of zinc phthalocyanine tetrasulfonic acid-functionalized graphene nanocomposites, Mater. Sci. Eng. C 49 (2015) 640–647.

[43] J. Kochana, K. Wapiennik, J. Kozak, P. Knihnicki, A. Pollap, M. Woźniakiewicz, J. Nowak, P. Kościelniak, Tyrosinase-based biosensor for determination of bisphenol A in a flow-batch system, Talanta 144 (2015) 163–170.

[44] Y. Li, H. Wang, B. Yan, H. Zhang, An electrochemical sensor for the determination of bisphenol A using glassy carbon electrode modified with reduced graphene oxide-silver/poly-L-lysine nanocomposites, J. Electroanal. Chem. 805 (2017) 39–46.

[45] D. Vega, L. Agüí, A. González-Cortés, P. Yáñez-Sedeño, J. Pingarrón, Electrochemical detection of phenolic estrogenic compounds at carbon nanotube-modified electrodes, Talanta 71 (2007) 1031–1038.

[46] Y. Li, X. Zhai, X. Liu, L. Wang, H. Liu, H. Wang, Electrochemical determination of bisphenol A at ordered mesoporous carbon modified nano-carbon ionic liquid paste electrode, Talanta 148 (2016) 362–369.

[47] Y. Zhou, L. Yang, S. Li, Y. Dang, A novel electrochemical sensor for highly sensitive detection of bisphenol A based on the hydrothermal synthesized Na-doped WO_3 nanorods, Sensor. Actuator. B Chem. 245 (2017) 238–246.

[48] R. Shi, J. Liang, Z. Zhao, A. Liu, Y. Tian, An electrochemical bisphenol A sensor based on one step electrochemical reduction of cuprous oxide wrapped graphene oxide nanoparticles modified electrode, Talanta 169 (2017) 37–43.

[49] K. Shim, J. Kim, M. Shahabuddin, Y. Yamauchi, M.S.A. Hossain, J.H. Kim, Efficient wide range electrochemical bisphenol-A sensor by self-supported dendritic platinum nanoparticles on screen-printed carbon electrode, Sensor. Actuator. B Chem. 255 (2018) 2800–2808.

[50] B. Su, H. Shao, N. Li, X. Chen, Z. Cai, X. Chen, A sensitive bisphenol A voltammetric sensor relying on AuPd nanoparticles/graphene composites modified glassy carbon electrode, Talanta 166 (2017) 126–132.

[51] F. Wang, J. Yang, K. Wu, Mesoporous silica-based electrochemical sensor for sensitive determination of environmental hormone bisphenol A, Anal. Chim. Acta 638 (2009) 23–28.

[52] T. Zhan, Y. Song, X. Li, W. Hou, Electrochemical sensor for bisphenol A based on ionic liquid functionalized Zn-Al layered double hydroxide modified electrode, Mater. Sci. Eng. C 64 (2016) 354–361.